

Waiting-time distributions of magnetic discontinuities: Clustering or Poisson process?

A. Greco*

Dipartimento di Fisica, Universita' della Calabria, I-87036 Cosenza, Italy

W. H. Matthaeus and S. Servidio†

Bartol Research Institute and Department of Physics and Astronomy, University of Delaware, Newark, Delaware 19716, USA

P. Dmitruk

Departamento de Física, Facultad de Ciencias Exactas y Naturales, Universidad de Buenos Aires, 1428 Buenos Aires, Argentina

(Received 4 July 2009; published 12 October 2009)

Using solar wind data from the Advanced Composition Explorer spacecraft, with the support of Hall magnetohydrodynamic simulations, the waiting-time distributions of magnetic discontinuities have been analyzed. A possible phenomenon of *clusterization* of these discontinuities is studied in detail. We perform a local Poisson's analysis in order to establish if these intermittent events are randomly distributed or not. Possible implications about the nature of solar wind discontinuities are discussed.

DOI: [10.1103/PhysRevE.80.046401](https://doi.org/10.1103/PhysRevE.80.046401)

PACS number(s): 52.35.Tc, 96.50.Bh, 94.05.Lk

I. INTRODUCTION

The statistical distribution of waiting time (WT) between “bursty” events is a powerful tool to investigate temporal pointlike processes such as, for example, solar flares, earthquakes, polarity reversals of geomagnetic field, stock market indexes, and lasing emissions in nematic liquid crystals [1–4]. Indeed, the shape of the probability distribution function for waiting times can give useful information about the physics of the underlying process. Another interesting case to study is the solar wind. This turbulent medium is characterized by the presence of strong small-scale magnetic fluctuations that behave as intermittent events [5–8]. There is still debate regarding the relative frequency and the nature of these intermittent signals. Some authors [9] have shown that the waiting times (interarrival times) between magnetic structures in the inner solar wind, measured by the Helios II satellite in interplanetary space at a distance $R=0.9$ AU from the sun, are distributed with a power law, extended over several decades. In fact, as turbulence may be viewed as a fragmentation process that carries energy from large to small scales, there exists a strong correlation between structures generated at different scales. This suggests that an underlying complex dynamics with long correlation times or “memory” is present [10].

There is also evidence that the probability density functions (PDFs) of waiting times are well described by exponential functions [5,6,11]. This exponential distribution is what would be expected if discontinuities occur with Poisson's statistics. Binomial or Poisson distributions (trivial statistics), in fact, imply no correlations between successive events, that is “lack of memory.” In another recent work [8], the distribution of separations between successive discontinuities has been described with a *log-normal* function. It has

been concluded that the results are potentially consistent with the exponential behavior even if the log-normal shape better characterizes the interarrival times over greater ranges. A log-normal distribution may indicate that turbulence in solar wind, which in principle can locally generate discontinuities [12], behaves like a multiplicative random cascade [8]. Indeed, the presence in the interplanetary magnetic field fluctuation spectrum of so-called “ $1/f$ ” noise at low frequencies has been explained by appeal to a multiplicative process lower in the corona [13]. Based on these considerations, one cannot rule out the possibility that correlations between successive bursty events are present.

In a comparative study on the waiting-time statistics governing the magnetohydrodynamic (MHD) fluctuations of the z component of the interplanetary magnetic field [14], it has been shown that the solar activity phase strongly influences the statistics which vary from quasi-Poisson to power law. Indeed, by comparing the obtained results, they found that the power-law behavior extends to longer time intervals at solar maximum than at minimum.

In situ solar wind measurements provide time series data at the position of the space craft. For MHD-scale fluctuations with velocities much smaller than the plasma bulk velocity V , the Taylor hypothesis is valid: the observed variations on a time scale δt correspond to variations on the spatial scale $\delta s = V \delta t$. Therefore the observations provide information about spatial structure. This allows meaningful comparisons of simulation and solar wind data sets. Recently [15], it was found through the analysis of Hall MHD simulations that distribution of WT between discontinuities for $s < \lambda_c$ is well described by a power law, while exponential functions work better for $s > \lambda_c$, where λ_c is the correlation length and s is the separation between suitably defined extreme events. Analysis of solar wind Advanced Composition Explorer (ACE) data [16] verified that power laws describe the distribution of WT for periods up to ~ 3000 s (50 min), which is on the order of the correlation length of magnetic fluctuations in the solar wind [17].

One needs to be cautious in concluding that the underlying process of cascade is non-Poissonian. Strong and signifi-

*greco@fis.unical.it

†Present address: Dipartimento di Fisica, Universita' della Calabria, I-87036 Rende (CS), Italy.

cant time variations have been found in the rate of occurrence of discontinuities from hour to hour, from day to day, and from solar rotation to solar rotation [5–8]. Regarding the solar rotation [6], it has been already pointed out that there is a high degree of persistence in the time variations: when high rates occur in a period of the solar activity, they are likely to be preceded and followed by high rates. A similar statement can be made about the low rates. Such variations can be shown to lie well outside the range permitted by simple Gaussian statistics. This may suggest that, although the rate of occurrence apparently obeys Poisson statistics on average, the rate is nonstationary and changes with time.

Several authors have suggested that a Poisson process with a variable rate, also called a *nonstationary* or *time-varying Poisson process*, can lead a power law for the WT distributions (see [1] for a more detailed explanation). In those cases, it is difficult to determine the Poisson character of events from the shape of the WT distribution and so is not easy to give a definite physical interpretation of the phenomenon [18]. To further clarify these issues, additional detailed analysis of temporal solar wind signals is warranted. We carry out such analysis here without any *a priori* assumptions on the Poisson's nature of the events.

The outline of the paper is as follows. We explain the method used as a zeroth-order test for the local Poisson hypothesis in Sec. II. In Sec. III, we show the WT distributions obtained through the analysis of ACE solar wind and Hall MHD simulation data. In Sec. IV, we apply the local Poisson's analysis directly on these time series. Finally, conclusions and possible implications for the nature of solar wind discontinuities will be discussed in Sec. V.

II. LOCAL POISSON HYPOTHESIS

Consider a physical process that occurs randomly in nature producing a stochastic temporal signal. Suppose now that we select “events” from the signal defined as values that exceed a specified threshold. The threshold is chosen arbitrarily, can vary with different methods, and depends on the physical problem. Each event has its own temporal duration; the waiting time Δt can be defined as the time interval between the end of an event and the beginning of the next one or between the beginnings of two successive events. If on average the durations of events are much shorter than the waiting times, it is possible to discard the duration of the single events and consider the signal as a pointlike process. This is equivalent to reducing each event to a single narrow peak, where the beginning and the ending of an event coincide and the waiting time between two consecutive events is simply the time difference between two peaks. The procedure mentioned above can reduce, for example, the time series of the magnetic discontinuities in the solar wind to a sequence of Dirac δ -function “events.”

A sequence of events that occurs randomly in time at a given mean rate λ follows Poisson statistics. The probability distribution of waiting times Δt is given by the exponential law

$$P(\Delta t) = \lambda e^{-\lambda \Delta t}, \quad (1)$$

typical of singular events that are “memoryless.” This means that, for $0 < t' < t$, $P(\Delta t > t | \Delta t > t') = P(\Delta t > t - t')$. In other

words, if Δt is equal to t' , the conditional probability of waiting for an event until a later time t is just the probability of waiting for a period of length $t - t'$. In this case, the process does not remember that it has already been running for a time t' . In contrast, if the probability distribution follows a power law, correlations are present [19].

Unfortunately, due to the limited size and the poor statistics of certain data set, sometimes it is not possible to obtain any useful information about the physics of the process from the PDFs of WT because they might suffer of some uncertainties. Moreover, the rate of appearance of isolated and intermittent events could be variable for several unknown reasons. When the occurrence rate is not constant, a situation often obtained in nature, these processes can be modeled as a realization of renewal Poisson processes with a variable rate, even if the distribution of separations cannot be used as a test to discriminate if the processes are Poissonian or not. For these reasons, without any *a priori* assumptions, a further analysis, less sensitive to the sample size and to the nonstationary character, can be performed. Such a method was introduced in cosmology by Bi *et al.* [20] in order to test the local Poisson hypothesis on Ly_α clouds in the absorption spectra of quasars. This method to test for local Poisson's statistics can be summarized as follows.

Suppose now that the pointlike process described before has a mean event rate $\lambda(t)$ that is neither constant nor known. Thus, we want to build up a test that is independent of λ [20,21]. This can be done through a measure that is nothing but the suitably normalized local time interval between events. Every event i has two nearest- and two next-nearest-neighbor events. We introduce the minimum local waiting time

$$\delta t_i = \min\{t_{i+1} - t_i, t_i - t_{i-1}\}, \quad (2)$$

while the next closest waiting time is given by

$$\delta \tau_i = \begin{cases} t_{i+2} - t_{i+1} & \text{if } \delta t_i = t_{i+1} - t_i \\ t_{i-1} - t_{i-2} & \text{if } \delta t_i = t_i - t_{i-1}. \end{cases} \quad (3)$$

In our specific case, δt_i and $\delta \tau_i$ can be two inter-event times before or after a magnetic discontinuity. We introduce now the stochastic variable H , that simply represents a normalized local time between bursty events, as

$$H(\delta t_i, \delta \tau_i) = \frac{\delta t_i}{\delta t_i + \frac{1}{2} \delta \tau_i}. \quad (4)$$

According to the local Poisson hypothesis, if δt_i and $\delta \tau_i$ are randomly distributed, the probability densities are, respectively,

$$P(\delta t_i) = 2\lambda_i e^{-2\lambda_i \delta t_i}, \quad (5)$$

$$P(\delta \tau_i) = \lambda_i e^{-\lambda_i \delta \tau_i}, \quad (6)$$

where λ_i is the local event rate. In this case, it can be easily shown that the stochastic variable H has a cumulative distribution $F(H)$ that is independent of λ ,

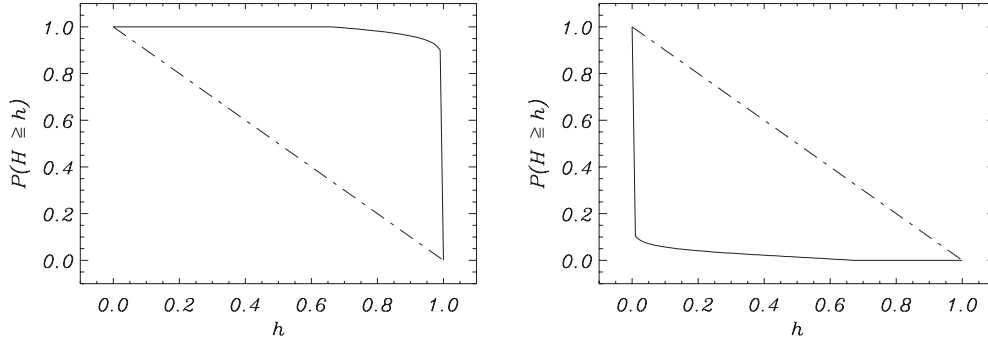


FIG. 1. Results of the test for local Poisson distribution performed on a process where $\delta t_i = a^i \delta \tau_i$ [see Eq. (8)], with $a=1.03$ (left panel) and $a=0.97$ (right panel). The dash-dotted line represents the curve $P(H \geq h) = 1 - h$ for a Poisson process. See Ref. [1] for more details.

$$F(H) = \int_0^H P(h) dh = \int_0^\infty dx 2\lambda e^{-2\lambda x} \int_0^{2x[(1/H)-1]} dy \lambda e^{-\lambda y} = 1 - H, \quad (7)$$

where $x = \delta t_i$, $y = \delta \tau_i$, and $[2x(1/H) - 1]$ is the y value derived from Eq. (4). This implies that, under the hypothesis that events are locally distributed with a Poisson statistic, the variable H is uniformly distributed between 0 and 1. In a process where $\delta \tau_i$ are systematically smaller than $2\delta t_i$, clusters are present and the average value of H is greater than $1/2$. On the contrary, when the process is characterized by the presence of voids, $H < 1/2$ [21].

As an example, consider a situation where $\delta t_i = a^i \delta \tau_i$, one then can easily obtain

$$H = \frac{2a^i}{2a^i + 1}. \quad (8)$$

If $a > 1$, events tend to cluster as i increases and $\lim_{i \rightarrow \infty} H = 1$, that is, H values are very close to 1. Conversely, if $a < 1$, events tend to separate as i increases and $\lim_{i \rightarrow \infty} H = 0$, which means that the great majority of H values are close to 0. If $a = 1$, that is, in a regular pattern where the magnetic discontinuities are placed with a constant average separation, H assumes the value $2/3$. The two situations, $a > 1$ and $a < 1$, are represented in Fig. 1.

Using Eq. (7) as a reference, this method can be used as a zeroth-order test for local Poisson hypothesis. For a pointlike process, given a sequence of observed events, the values of the variable H can be easily calculated and the probability $P(H \geq h)$ to find a value $H \geq h$ for a fixed h [$F(H)$ in the Eq. (7)] can be computed and compared to the Poisson behavior $1 - h$.

III. DISCONTINUITIES IN TURBULENCE: SOLAR WIND AND SIMULATION DATA

In this section, we review briefly the methods used to identify magnetic discontinuities, defined by large changes in the magnitude of the magnetic field vector increments $|\Delta_{\Delta s} \mathbf{B}| = |\mathbf{B}(s + \Delta s) - \mathbf{B}(s)|$ at the scale Δs [6]. We will employ solar wind data from the ACE spacecraft [16], as well as data from three-dimensional (3D) Hall MHD numerical simulations [15].

The compressible Hall MHD equations are given by

$$\frac{\partial \rho}{\partial t} + \nabla \cdot (\rho \mathbf{v}) = 0, \quad (9)$$

$$\frac{\partial \mathbf{v}}{\partial t} + (\mathbf{v} \cdot \nabla) \mathbf{v} = -\frac{1}{\rho \gamma M_s^2} \nabla p + \frac{\mathbf{j} \times \mathbf{b}}{\rho} + \frac{1}{R_\nu} \left[\nabla^2 \mathbf{v} + \frac{1}{3} \nabla (\nabla \cdot \mathbf{v}) \right], \quad (10)$$

$$\frac{\partial \mathbf{b}}{\partial t} = \nabla \times (\mathbf{v} \times \mathbf{b}) - \epsilon \nabla \left(\frac{\mathbf{j} \times \mathbf{b}}{\rho} \right) + \frac{1}{R_\mu} \nabla^2 \mathbf{b}, \quad (11)$$

where p is the pressure and $\mathbf{j} = \nabla \times \mathbf{b}$. For the pressure, we assume a polytropic case $p = p_0 (\frac{\rho}{\rho_0})^\gamma$, where ρ_0 and p_0 are initial density and pressure, respectively. The adiabatic index $\gamma = 5/3$. The above equations are written in the usual Alfvénic dimensionless form based on a characteristic plasma Alfvén speed $v_a = b_{\text{rms}} / \sqrt{4\pi \rho_0}$, where $b_{\text{rms}} = \langle B^2 \rangle^{1/2}$ is the root-mean-square (rms) magnetic field, a characteristic length scale L_0 (the simulation box is set to be $2\pi L_0$), and a unit time scale $t_a = L_0 / v_a$. The dimensionless numbers that appear here are the Mach number $M_s = v_a / c_s$, where $c_s = \sqrt{\gamma p_0 / \rho_0}$ is the sound speed, the Reynolds number $R_\nu = v_a L_0 / \nu$ (ν is the viscosity), and the magnetic Reynolds number $R_\mu = v_a L_0 / \mu$, with $c^2 \eta / (4\pi)$ the magnetic diffusivity. The Hall parameter $\epsilon = \rho_{ii} / L_0$, with $\rho_{ii} = c / \omega_{pi}$ the ion skin depth (or ion inertial length) and ω_{pi} the plasma frequency. The coefficient ϵ appears in front of the Hall term in the normalized equations, expressing the fact that the Hall term becomes important at scales smaller than the ion skin depth ρ_{ii} . 3D Hall MHD simulations are carried out using a Fourier pseudospectral method in a periodic box of side $2\pi L_0$ and 256^3 spatial grid points. More details on the code and the simulations are given in Refs. [15,16].

The available solar wind data set includes 16 s averages of the magnetic field vector. The time interval spanned 135 days (five Bartels rotation) during 2001. In a previous work (for more details, see Ref. [15]), in an analysis of Hall MHD simulation data, we examined the relationship between discontinuities, identified by a classical method [5,6], called the Tsurutani and Smith (TS) method, and coherent structures identified by intermittency statistics, called the partial vari-

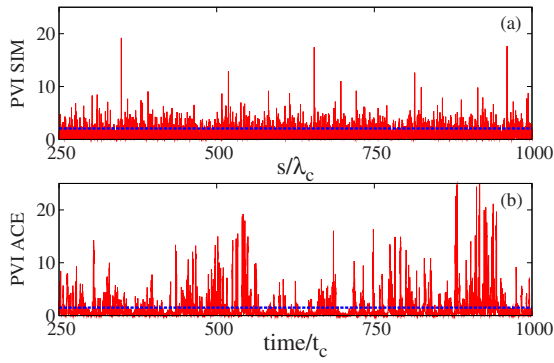


FIG. 2. (Color online) (a) Spatial distribution of magnetic discontinuities computed from simulation vs distance s/λ_c at $\Delta s = 0.006\ 25\lambda_c$ (solid-thin red line). (b) Time series (normalized to correlation time t_c) of discontinuities computed from ACE data. Events are selected according to the PVI method [15,16] and the thick dashed blue lines are the values of the thresholds. We show only a portion of the entire data set.

ance of increments (PVI) method. An example of time series of these intermittent events is shown in Fig. 2, computed from numerical simulations at $\Delta s = 0.006\ 25\lambda_c$ (the most intermittent scale of the simulation) and from solar wind data at $\Delta s = 4$ min, and selected according to the PVI technique. It has been found that the two methods produce remarkably similar distributions of waiting times. For the simulation, a spatial sampling along a line was employed. For the solar wind, a time series of data was employed. There is a direct analogy between these simulation and solar wind cases. A spacecraft time series that satisfies Taylor’s hypothesis—the sampling time of solar wind fluctuations is much less than the time scale on which they vary—can be considered a spatial “snapshot” of the plasma. The distance between consecutive events s has been normalized to the correlation length of the turbulent field λ_c in the simulation and analogously for the solar wind, we normalize time to the correlation time $t_c \approx 50$ min.

In Fig. 2, we compare the solar wind signal and the simulation for the same number of correlation lengths. It can be seen that the two signals have some similar features, but also differences. The dissimilarities between simulations and real solar wind data can be associated with many factors: time dependency, finite Reynolds number, limits of the fluid approximation, different driving, anisotropy, and so on. On the other hand, as described in an earlier work [16], both signals are bursty, suggesting that some features of these intermittent events can be captured by models of fully developed MHD turbulence.

Some results on the distribution of waiting times are summarized in Fig. 3. For $s < \lambda_c$, the distributions are both well described by a power law $\sim s^{-0.92}$, while the exponential works well for $s > \lambda_c$. A similar analysis has been performed on the solar wind turbulent magnetic field [16] with similar results. We computed waiting-time distributions of large changes in the magnitude of the magnetic field vector increment at separations lying in the inertial range for ACE solar wind data. Using the intermittency (PVI) and discontinuity (TS) analyses, we found that the performance of the two

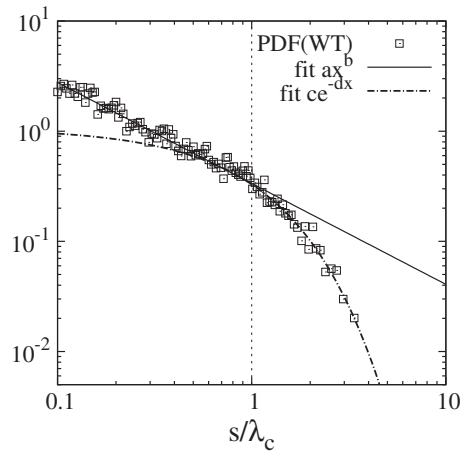


FIG. 3. Distribution of waiting times in the Hall MHD simulation (squares), detected by a classical analysis (TS method) at $\Delta s = 0.006\ 25\lambda_c$. The power-law ax^b (solid line) and the exponential ce^{-dx} (dash-dotted line) fits are also shown. The parameters and the errors of the fits are $a = 0.34 \pm 0.01$ and $b = -0.92 \pm 0.03$; $c = 1.1 \pm 0.1$ and $d = 1.18 \pm 0.06$. Vertical dashed line is placed at one correlation length.

methods is comparable for solar wind data as well as for simulation data. In Fig. 4, the PDFs of WT between the events identified by the implementation of TS and PVI methods are shown. The technique gives very similar results up to ~ 1000 s. Their respective fits show that, for both cases, the power laws break at $\sim 1000\text{--}3000$ s [14]. These power-law waiting times could be clear evidence that long-range correlations are present in the underlying MHD turbulent cascade process. To gain insight regarding this apparent clusteriza-

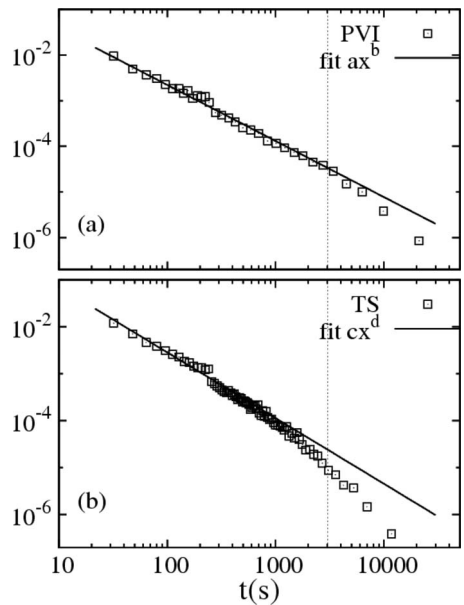


FIG. 4. Distributions of waiting times between discontinuities detected in solar wind (open squares) using (a) the PVI method and (b) the TS classical technique. Solid lines represent the power-law fits. The parameters and the errors of the fits are $a = 0.64 \pm 0.08$ and $b = -1.23 \pm 0.03$; $c = 1.8 \pm 0.06$ and $d = -1.4 \pm 0.04$. Vertical lines indicate the correlation time of 50 min.

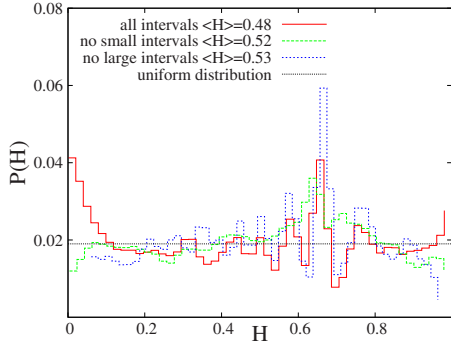


FIG. 5. (Color online) $P(H)$ for the local Poissonian test, performed on solar wind data (ACE data set). Data are selected with the PVI method with different criteria, namely, all the events are taken into account (full red line), WTs with $\delta t < 10^3$ s (dotted blue line), and $\delta t > 100$ s (dashed green line). The uniform probability in $[0,1]$ (thin dotted black line), expected under a Poisson statistics, is also shown and the average values of the stochastic variable $\langle H \rangle$ are reported as well.

tion, in the next section we examine the local Poisson hypothesis for both Hall MHD and solar wind discontinuities.

IV. LOCAL POISSON HYPOTHESIS FOR THE DISCONTINUITIES OCCURRENCE

We can test, as a zeroth-order hypothesis (say, H_0), whether an approach based on the occurrence of a local Poisson process, given by Eq. (7), is appropriate or not. In other words, it can be conjectured that an underlying time-varying Poisson process produces discontinuities in a magnetofluid turbulence and, analogously, in solar wind plasma. This can be done by using the method introduced in Sec. II.

We analyze the same time sequence used for the WT-diagnostic performed before. We verified that, on average, the duration times of bursts are much smaller than the waiting times between the bursts. With this assumption, we can consider the discontinuities as pointlike events. The values of H have been calculated from these data sets. In Fig. 5, we show the PDFs $P(H)$ calculated with the discontinuities detected from ACE using the PVI method. Three different cases are shown: waiting times with all the data, the case in which we exclude waiting times that last less than < 100 s (small intervals), and the case in which we filter out discontinuities with a delay $> 10^3$ s (large intervals). It is clear that the statistics are sensitive to which types of events we consider: when all duration waiting times are taken into account $\langle H \rangle < 1/2$, indicating a weak attenuation of the discontinuities with time (or distance). On the contrary, when “small” or “large” scale WTs are discarded, clusters are present ($\langle H \rangle > 1/2$). When we use TS method, the $P(H)$ is also sensitive to temporal scale of the included WTs, but at a lesser extent. As it can be seen from Fig. 5, in every case, $P(H)$ is very different from the uniform distribution. This supports the

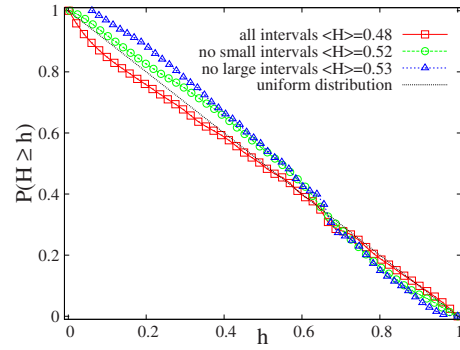


FIG. 6. (Color online) Cumulative PDF for solar wind data selected with the PVI method. As in Fig. 5, we filter out different waiting-time ranges: all the events (full red line and squares), WTs with $\delta t < 10^3$ s (dotted blue line and triangles), and $\delta t > 100$ s (dashed green line and circles). The thin dotted black line represents $P(H \geq h) = 1 - h$ that describes a Poisson process.

hypothesis that the statistical behavior of the events departs from a Poisson’s expectation.

From $P(H)$, we computed the cumulative probability density function (CPDF) $P(H \geq h)$ which we compare to the linear law $1 - h$ [in Eq. (7)] expected under the hypothesis H_0 . The results, for the three cases mentioned above, are shown in Fig. 6. Note that all three lines cross the dotted line $1 - h$ that describes a Poisson process close to the value $h = 2/3$. As explained in Sec. II, $h = 2/3$ divides events that tend to cluster from events that tend to separate as the time increases. This crossing at $h = 2/3$ is observable for all the CPDFs displayed in the following figures. A Kolmogorov-Smirnov (KS) test applied to the cumulative distributions confirms that the assumed hypothesis H_0 is not reliable for the cases in which we exclude waiting times that last less than < 100 s and in which we filter out discontinuities with a delay $> 10^3$ s (the probabilities that the processes are Poissonian being 10% and 28%, respectively). When we consider the case of waiting times of all duration, the KS test gives a significance level of 37%, meaning that an underlying Poisson process could be still possible. We compare the PVI and

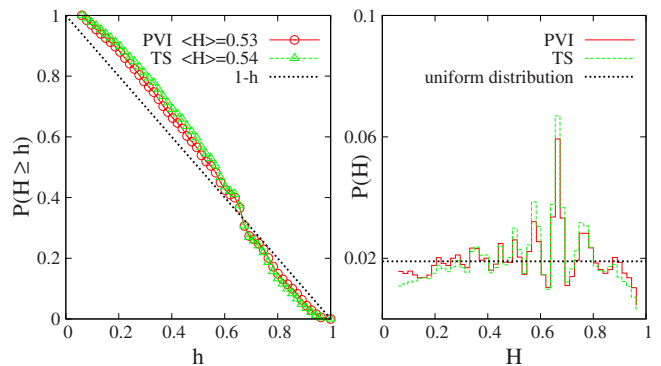


FIG. 7. (Color online) Left: CPDFs from the test for local Poisson distribution for both PVI (solid red line and circles) and TS (dashed green line and triangles). As in Fig. 6, the dotted (black) line represents the Poisson expectation $1 - h$. Right: $P(H)$ for the PVI (solid red line) and TS (dashed green line) methods, together with the uniform probability in $[0,1]$ (dotted black line).

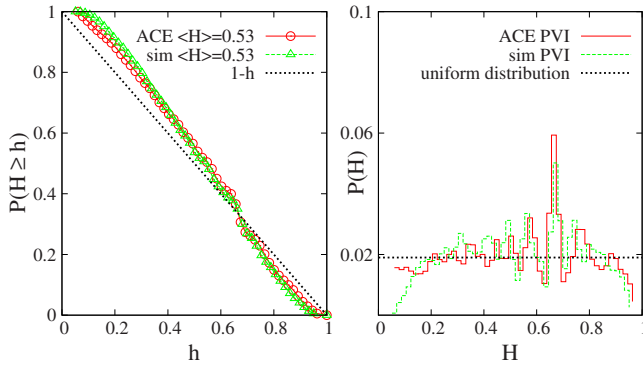


FIG. 8. (Color online) Comparison between the Hall MHD simulation and the solar wind ACE data using the PVI method. Left: CPDFs for ACE data (solid red line and circles) and for the simulation (dashed green line and triangles). Right: $P(H)$ for the solar wind (solid red line) and the simulation (dashed green line). See captions of Figs. 5–7 for more details.

TS methods in Fig. 7, where $P(H)$ and $P(H \geq h)$ are both shown. The agreement is good when we neglect waiting times between discontinuities that are greater than $>10^3$ s (where the power laws break, as shown in Fig. 4). The KS test applied to the CPDF for solar wind data, selected with the TS method, rejects the hypothesis H_0 because the probability for an underlying Poissonian process is equal to 3%.

We perform the local Poissonian test on the discontinuities detected from the Hall MHD simulations considered in [15] and compare $P(H \geq h)$ and $P(H)$ to those obtained from the analysis on the solar wind discontinuities. The comparison is displayed in Fig. 8 for the PVI method (neglecting large WTs). In this case, the KS test gives a probability of underlying Poisson processes in the Hall MHD simulation equal to 4%. The results obtained with TS classical criteria (not shown) are almost the same. It is clear that Poisson statistics cannot account for the waiting-time distributions of discontinuities either in the solar wind data set or in the simulations. Long-range correlations between bursts could be the origin of the power law for waiting times.

As a further test for the goodness of the procedure and in order to measure the “non-Poissonianity” of the data set, we make use of a randomization technique. We have built up a sample through a randomization of the measured magnetic field from ACE spacecraft with Gaussian distributions while retaining the same (average) spectrum and then we have detected a certain number of discontinuities by implementing, e.g., the PVI method. That is, we consider a time interval that covers the same duration as the experimental data set, with a number of “random” discontinuities from a phase-randomized reference magnetic field. This procedure is a powerful tool that permits us to obtain from a sample of data another similar data set, but one that lacks any clustering. The analysis performed on the hybrid data set gives a Poissonian curve $P(H \geq h) = 1 - h$ (as shown in Fig. 9) with a significance level equal to 85%. This result supports the presence of large scale correlations in the original unmodified solar wind data set.

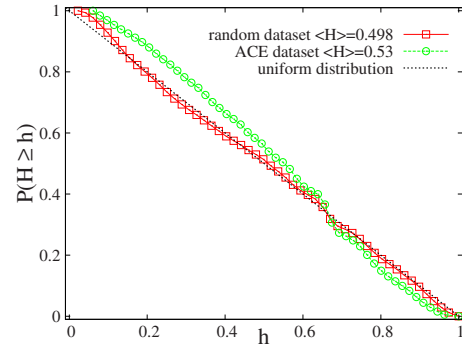


FIG. 9. (Color online) The CPDFs computed for the solar wind (solid red line and squares) and for a random sample (dashed green line and circles). Dotted black line represents the Poisson expectation $1-h$.

V. DISCUSSIONS AND CONCLUSIONS

Using solar wind data from the ACE spacecraft, along with data from Hall MHD simulation, we have analyzed the waiting times between suitably defined magnetic discontinuities. With these discontinuities regarded as short (zero) time-thickness events, we found, first, that the statistical results are not strongly dependent on the method employed for the identification of these events. Classical methods gave very similar results to methods based on intermittency analysis [15,16]. Second, we found that the distribution of waiting times is better described as a power law for spatial separation scales less than the correlation scale, while waiting times that correspond to events separated by more than a correlation scale were better described as an exponential (Poisson) distribution for both the Hall MHD simulations and the solar wind data. For the waiting times between solar wind discontinuities, we found that the power law breaks at the typical correlation scale in the solar wind and is exponential at longer waiting times. This conclusion appears to be unaffected by the remnant low-frequency correlations associated with coronal processes such as those that produce $1/f$ noise [13].

The test for Poisson processes introduced by [20] was employed to further examine the distribution of waiting time for these events. The tests showed that the discontinuities are not distributed without correlations, but rather that non-Poisson correlations, possibly in the form of burstiness or voids, are present in the data at least up to the typical correlation scale. A similar conclusion emerges from Poisson analysis of the simulation data set. Our tentative conclusion is that Poisson’s random noise might well characterize the very large scale solar wind fluctuations. However in the inertial range (scales $<$ a few hours in the spacecraft frame), the analysis suggests the presence of correlations and the waiting times between events display an associated bursty character. This supports the viewpoint that solar wind turbulent fluctuations at least in part are related to the presence of large structures of highly conducting plasma. The discontinuities or bursty coherent structures represent in this view the current sheets that form between magnetic-flux tubes [22–24] which may be a signature of intermittent, anisotropic, fully developed MHD turbulence.

ACKNOWLEDGMENTS

This research supported in part by the NASA Heliophysics Theory Program No. NNX08AI47G, by U.S. NSF Grant No. ATM0752135, and by Italian Space Agency, Contract

ASI No. I/015/07/0 “Esplorazione del Sistema Solare.” We acknowledge A. Vecchio, V. Carbone, L. Sorriso-Valvo, and F. Lepreti for helpful suggestions and discussions. We thank Lorenzo Servidio for his valuable cooperation.

-
- [1] F. Lepreti, V. Carbone, and P. Veltri, *Astrophys. J.* **555**, L133 (2001).
- [2] V. Carbone, L. Sorriso-Valvo, A. Vecchio, F. Lepreti, P. Veltri, P. Harabaglia, and I. Guerra, *Phys. Rev. Lett.* **96**, 128501 (2006).
- [3] A. Greco, L. Sorriso-Valvo, V. Carbone, and S. Cidone, *Physica A* **387**, 4272 (2008).
- [4] S. Ferjani, L. Sorriso-Valvo, A. De Luca, V. Barna, R. De Marco, and G. Strangi, *Phys. Rev. E* **78**, 011707 (2008).
- [5] L. F. Burlaga, *Sol. Phys.* **7**, 54 (1969).
- [6] B. T. Tsurutani and E. J. Smith, *J. Geophys. Res.* **84**, 2773 (1979).
- [7] T. Knetter, F. M. Neubauer, T. Horbury, and A. Balogh, *J. Geophys. Res.* **109**, A06102 (2004).
- [8] B. J. Vasquez, V. I. Abramenko, D. K. Haggerty, and C. W. Smith, *J. Geophys. Res.* **112**, A11102 (2007).
- [9] V. Carbone, L. Sorriso-Valvo, F. Lepreti, P. Veltri, and R. Bruno, in *Solar Wind Ten*, AIP Conf. Proc. Vol. 679, edited by M. Velli, R. Bruno, F. Malara, and B. Bucci (AIP, New York, 2003).
- [10] R. Bruno and V. Carbone, *Living Rev. Solar Phys.* **2**, 4 (2005).
- [11] R. Bruno, V. Carbone, P. Veltri, E. Pietropaolo, and B. Bavassano, *Planet. Space Sci.* **49**, 1201 (2001).
- [12] S. Servidio, W. H. Matthaeus, M. A. Shay, P. A. Cassak, and P. Dmitruk, *Phys. Rev. Lett.* **102**, 115003 (2009).
- [13] W. H. Matthaeus and M. L. Goldstein, *Phys. Rev. Lett.* **57**, 495 (1986).
- [14] R. D’Amicis, R. Bruno, B. Bavassano, V. Carbone, and L. Sorriso-Valvo, *Ann. Geophys.* **24**, 2735 (2006).
- [15] A. Greco, P. Chuychai, W. H. Matthaeus, S. Servidio, and P. Dmitruk, *Geophys. Res. Lett.* **35**, L19111 (2008).
- [16] A. Greco, W. H. Matthaeus, S. Servidio, P. Chuychai, and P. Dmitruk, *Astrophys. J.* **691**, L111 (2009).
- [17] W. H. Matthaeus, S. Dasso, J. M. Weygand, L. J. Milano, C. W. Smith, and M. G. Kivelson, *Phys. Rev. Lett.* **95**, 231101 (2005).
- [18] W. Feller, *An Introduction to Probability Theory and its Applications*, 2nd ed., Wiley Series in Probability and Mathematical Statistics (Wiley, New York, 1968).
- [19] G. Boffetta, V. Carbone, P. Giuliani, P. Veltri, and A. Vulpiani, *Phys. Rev. Lett.* **83**, 4662 (1999).
- [20] H. Bi, G. Boerner, and Y. Chu, *Astron. Astrophys.* **218**, 19 (1989).
- [21] A. Vecchio, V. Carbone, L. Sorriso-Valvo, C. De Rose, I. Guerra, and P. Harabaglia, *Nonlinear Processes Geophys.* **15**, 333 (2008).
- [22] P. Veltri, *Plasma Phys. Controlled Fusion* **41**, A787 (1999).
- [23] S. Servidio, W. H. Matthaeus, and P. Dmitruk, *Phys. Rev. Lett.* **100**, 095005 (2008).
- [24] J. E. Borovsky, *J. Geophys. Res.* **113**, A08110 (2008).